

PACS numbers: 85.70.Sq
DOI: 10.1070/QE2006v036n04ABEH013154

Considerable reduction of thermooptical distortions in Faraday isolators cooled to 77 K

D.S. Zheleznov, A.V. Voitovich, I.B. Mukhin, O.V. Palashov, E.A. Khazanov

***Abstract*. It is shown experimentally that cooling of a Faraday isolator to liquid nitrogen temperature considerably suppresses the thermally induced depolarisation and reduces the thermal lens. This leads to an increase in the maximum average laser radiation power passing through the isolator by a factor of more than thirty for the same degree of isolation. It is shown that for the same level of cooling, conventional Faraday isolators can operate for powers up to 10 kW, while isolators with compensation of depolarisation and thermal lens can operate up to 100 kW.**

Keywords: *thermal lens, depolarisation, thermal optics, Faraday effect*.

1. Introduction

The compensation of thermal effects arising in various optical elements due to absorption of laser radiation has acquired significance following an intense growth of laser technology and an increase in the average power of cw as well as repetitively pulsed laser regimes. One of the devices in which the laser radiation is subjected to a strong thermal self-action is a Faraday isolator (FI) on account of intense absorption of radiation by its magneto-optical elements ($\sim 10^{-3}$ cm^{-1}) [1]. The absorption-induced nonuniform temperature distribution over the cross section leads to a nonuniform distribution of the angle of rotation of the polarisation plane (associated with the temperature dependence of the Verdet constant), to the emergence of linear birefringence (photoelastic effect) [2] and to a distortion of the wavefront of optical radiation passing through an FI (thermal lens).

The temperature dependence of the Verdet constant and the photoelastic effect change the radiation polarisation, which lowers the degree of isolation of the FI. The aberrations caused by a thermal lens do not lead to polarisation distortions, but affect the mode composition of optical radiation passing through the FI. In some applications (e.g., the detection of gravitational waves using laser interferometers [3]), the power losses in the fundamental transverse mode must not exceed 1 % – 2 %. Several publications, including [4 – 7], have been devoted to the compensation of a thermal lens in an FI. The possibility of compensating a thermal lens with the help of a misaligned lens telescope was considered in [4]. Moreover, a thermal lens can be compensated by using an absorbing glass [5, 6] or crystal [7] with a negative value of dn/dT (n is the refractive index and T is the temperature).

The degree of isolation, which is an important parameter of an FI, is mainly determined by polarisation distortions, i.e., the magnitude of depolarisation in magnetically active elements. The 'cold' depolarisation emerging in magnetically active elements due to inhomogeneity and imperfection of an optical element (streaks, crystal lattice imperfections, etc.) is small as a rule ($10^{-5} - 10^{-4}$). Depolarisation, caused by radiation absorption in optical elements and called 'hot' or 'thermally induced' depolarisation depends considerably on the optical radiation power and may be significantly higher than cold depolarisation.

Several methods have been proposed for decreasing the thermally induced depolarisation in magnetically active elements of FIs. One such approach is based on the idea of withholding the phase delay by replacing a Faraday element rotating the polarisation plane through 45° by two 22.5° Faraday elements with a reciprocal optical element between them [2, 8]. The distortions arising during passage through the first element are partly compensated during passage through the second element. The FI and Faraday mirrors fabricated on the basis of such elements [9, 10] ensure a reliable isolation for a kilowatt-level power of the radiation being transmitted. Another approach involves splitting of the magnetically active element into a number of thin discs cooled through the optical surface [11, 12]. Such a geometry considerably lowers the transverse temperature gradient in the discs. Theoretical estimates show that a transition from rod geometry to the disc geometry leads to the production of FIs working in the radiation power range of ten kilowatts [11].

In this paper, we propose yet another method of improving the parameters of Faraday isolators by cooling them down to liquid nitrogen temperature. Note that cooling of the active elements of lasers is widely used for increasing the thermal conductivity and the gain [13 – 15]. Because the Verdet constant is inversely proportional to temperature [16 – 18] and the magnetic field also increases upon cooling of the magnetic system [19 – 21], it can be

D.S. Zheleznov, A.V. Voitovich, I.B. Mukhin, O.V. Palashov, E.A. Khazanov Institute of Applied Physics, Russian Academy of Sciences, ul. Ul'yanova 46, 603950 Nizhnii Novgorod, Russia; e-mail: khazanov@appl.sci-nnov.ru

Received 26 December 2005
Kvantovaya Elektronika **36** (4) 383 – 388 (2006)
Translated by Ram Wadhwa

expected that the length of the magnetically active element will decrease and hence all thermal effects can be suppressed.

We shall present here the results of experimental study of thermally induced depolarisation, thermal lens, Verdet constant and the magnetic field upon cooling the FI elements to temperatures close to the liquid nitrogen temperature. For the magnetically active media, we used the MOS04 glass [1] and a terbium gallium garnet (TGG) crystal with a [001] orientation. The investigations carried out by us hint at the possibility of fabricating an FI operating at an average power of right up to 100 kW.

2. Temperature dependence of thermally induced depolarisation

It was shown in [2, 22] that the dominating contribution to thermally induced depolarisation comes from the photoelastic effect, while the temperature dependence of the Verdet constant can be neglected. This section is devoted to a study of thermally induced depolarisation associated with the photoelastic effect.

Figure 1a shows the scheme of the experimental setup. Polarised cw 1076-nm radiation from single-mode ytterbium-doped fibre laser (*1*) was used simultaneously for heating and probing. The beam radius r_0 for radiation power up to 50 W was $\sim$0.5 mm. Radiation from laser (*1*) was directed to vacuum cryostat (*2*) through input window (*3*) made of fused silica. The cryostat is a vacuum chamber in a doubly cooled vessel: the inner part of the vessel is in direct thermal contact with the sample under investigation while the outer one is intended for additional cooling of the inner vessel and slows down the evaporation of the coolant in it to such an extent that cooling of the magnetically active element can be made quasi-stationary. Cooling of the magnetically active element was monitored by a calibrated temperature-sensitive copper element. After passing through calcite wedge (*4*), linearly polarised radiation fell on magnetically active element (*5*) under investigation. Heating of the magnetically active medium due to absorption led to depolarisation of radiation which was split into two parts by calcite wedge (*6*). The main part of radiation having power P_2 was extracted from the cryostat through output window (*7*) made of fused silica and fell on absorber (*8*), while the depolarised component having power P_1 was directed to CCD camera (*9*).

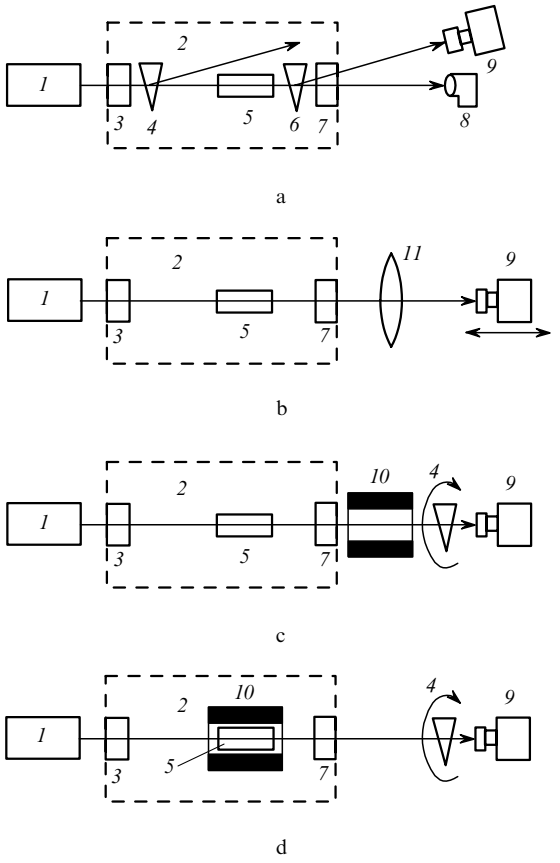

Figure 1. Scheme of experiments for studying (a) depolarisation, (b) thermal lens, (c) Verdet constant and (d) magnetic field: (*1*) ytterbium-doped fibre laser; (*2*) cryostat; (*3*, *7*) cryostat windows; (*4*, *6*) calcite wedges; (*5*) magnetically active element; (*8*) absorber; (*9*) CCD camera; (*10*) magnet; (*11*) calibrated lens.

Thermally induced depolarisation γ can be defined as

$$\gamma = \frac{P_1}{P_1 + P_2}. \tag{1}$$

Cold depolarisation in the magnetically active elements used in this study was insignificant ($\sim 10^{-5}$). Cryostat windows (*3*) and (*7*) virtually do not absorb laser radiation but the stresses emerging in them due to atmospheric pressure cause a certain depolarisation ($\sim 10^{-3}$) of the radiation passing through them. In order to avoid the parasitic influence of this effect on the results of measurements, calcite wedges (*4*) and (*6*) were mounted inside the cryostat.

Thermally induced depolarisation emerging due to the photoelastic effect was studied in detail in a number of works [2, 22, 23]. For example, an expression for depolarisation in a TGG crystal with orientation [001] was obtained in [22]:

$$\gamma = p^2 \frac{A}{8}\left[1 + \left(\xi^2 - 1\right)\cos^2\left(2\theta - \frac{\pi}{4}\right)\right], \tag{2}$$

where

$$p = \frac{L}{\lambda}\frac{\alpha Q}{\kappa} P_L \tag{3}$$

is the intensity of the photoelastic effect; L is the length of the magnetically active element; α and κ are the absorption coefficient and the thermal conductivity; λ and P_L are the wavelength and power of the transmitted radiation; Q is the thermo-optical constant [24]; $A = 0.137$ is a constant for the Gaussian distribution of the transmitted radiation [2]; θ is the angle between the radiation polarisation and the crystallographic axis of the crystal;

$$\xi = \frac{2p_{44}}{p_{11} - p_{12}} \tag{4}$$

is the optical anisotropy parameter [24]; and p_{ij} are the photoelastic constants.

It can be seen from expression (2) that thermally induced depolarisation γ is independent of θ for magnetically active glass elements since $\xi = 1$. For a crystal with orientation

Table 1. Material constants of magnetically active media.

Material	$\alpha/10^{-3}$ cm^{-1}	κ/W K^{-1} m^{-1}	$L^{-1}\frac{dL}{dT}\Big/10^{-7}$ K^{-1}	$\frac{P}{\kappa}\Big/10^{-6}$ m W^{-1}	$\frac{Q}{\kappa}\Big/10^{-7}$ m W^{-1}	ξ	V/deg kOe^{-1} cm^{-1}
TGG	9.6 ($\lambda = 1076$ nm) 4.8 ($\lambda = 1053$ nm)	7.4 [5, 6, 28, 29] 5.3 ± 0.5 [30] 4.5 ± 0.5 [27] 4.3 [31]	94 [29]	3.5 [6]	3.5 [6]	2.25 ± 0.2 [6, 23]	2.2 ($\lambda = 1076$ nm) 2.25 ($\lambda = 1064$ nm)
MOS04		0.74 [32]	49 [33]		12 [32]	1	1.21 ($\lambda = 1076$ nm) 1.24 ($\lambda = 1064$ nm)

[001], the depolarisation γ depends on the angle θ and assumes the following highest (γ_{max}) and lowest (γ_{min}) values:

$$\gamma_{max} = p^2 \frac{A}{8}\xi^2, \quad \gamma_{min} = p^2 \frac{A}{8}. \tag{5}$$

We studied the temperature dependence of thermally induced depolarisation γ in the magnetically active glass MOS04 of length 31 mm and diameter 8.3 mm, and in a TGG crystal with orientation [001] (length 47 mm and diameter 9 mm). Table 1 contains the values of a number of constants for these samples at room temperature $T_0 = 293$ K. However, their behaviour upon a lowering of the medium temperature had not been studied earlier, and hence it was hard to predict the behaviour of the thermally induced depolarisation.

Figure 2 shows the experimental dependences of the normalised depolarisation

$$\gamma_{norm}(T) = \frac{\gamma(T)}{\gamma_0}, \tag{6}$$

where $\gamma_0 = \gamma(T_0)$. Experimental results show that cooling of the TGG crystal to a temperature of 86 K lowers the depolarisation γ_{min} by a factor of 8. It was shown in [22] that the expression for depolarisation in a conventional FI coincides with the expressions (2) and (5) if the coefficient 1/8 is replaced by π^{-2}. Consequently, an eightfold decrease in the value of γ_{min} also increases isolation by a factor of 8. Moreover, it follows from (5) that the parameter $\alpha Q/\kappa$ decreases by a factor of $\sqrt{8}$. One can see from Fig. 2 that γ_{max} decreases by a factor of more than 24 upon cooling; in other words, the optical anisotropy parameter ξ decreases by a factor of $\sqrt{3}$ in accordance with expressions (5).

Cooling of the MOS04 sample to a temperature of 82 K reduces the depolarisation to nearly one third of its value, which means that the quantity $\alpha Q/\kappa$ for glass decreases by a factor of $\sim\sqrt{3}$ upon cooling.

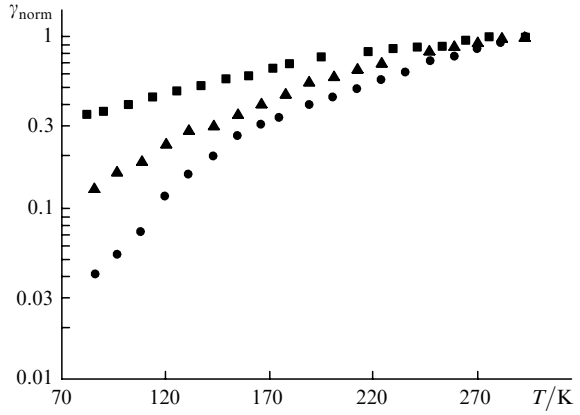

Figure 2. Temperature dependence of normalised thermally induced depolarisation γ_{norm} in a TGG crystal with orientation [001] in positions with maximum (dark circles, $\gamma_0 = 3.1 \times 10^{-2}$, $P_L = 35$ W) and minimum (dark triangles, $\gamma_0 = 5.2 \times 10^{-3}$, $P_L = 35$ W) depolarisations, as well as in the MOS04 glass (dark squares, $\gamma_0 = 5.1 \times 10^{-3}$, $P_L = 50$ W).

3. Temperature dependence of the optical power of a thermal lens

A high-power laser radiation beam passing through an absorbing optical element experiences a wavefront distortion due to a nonuniform temperature distribution over the cross section of the element. The experimental setup for measuring the temperature dependence of the optical power of a thermal lens is shown in Fig. 1b. Radiation from 15–20-W single-mode ytterbium-doped fibre laser (*1*) passed through magnetically active element (*5*) inside vacuum cryostat (*2*), from where it was directed to CCD camera (*9*) after passing the calibrated condensing lens (focal length $F_1 = 516$ mm). The CCD camera was displaced along the beam at each value of temperature. Knowing the position of the camera at which the beam was the narrowest, we calculated the focal length of the thermal lens of the magnetically active element using the known coordinate dependence of the Gaussian beam diameter.

Figure 3 shows the temperature dependence of the normalised optical power $1/F_{norm}$, where

$$F_{norm}(T) = \frac{F(T)}{F_0}, \quad F_0 = F(T_0).$$

As the temperature is lowered to 102 K, the optical power of the lens in the TGG crystal decreases by a factor of 2.7, which means that a 3.6-fold decrease can be expected at liquid nitrogen temperature (77 K). Since the transverse

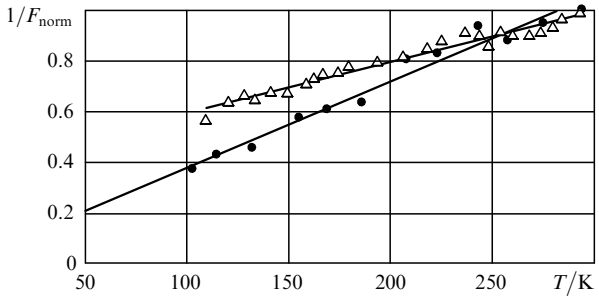

Figure 3. Temperature dependence of the optical power of a thermal lens in a TGG crystal with orientation [001] (dark circles, $F_0 = 191$ cm, $P_L = 15$ W) and in the MOS04 glass (triangles, $F_0 = 581$ cm, $P_L = 20$ W).

distribution of the heating radiation intensity is Gaussian, the temperature distribution is not parabolic and hence the induced thermooptical lens is aberrational. Such a lens can be presented as a set of two elements, namely, a parabolic lens of focal length F and an aberrator that does not introduce any geometrical divergence. Using the method of moments described in [25], we obtain a simple expression for F [26]:

$$F = \frac{4\pi r_0^2}{\lambda p_i}, \tag{7}$$

where

$$p_i = \frac{L}{\lambda}\frac{\alpha P}{\kappa}P_L \tag{8}$$

is the optical power of the thermal lens, and P is the thermo-optical constant [24]. Note that the parameter p_i is analogous to the parameter p in (3), except that the thermo-optical constant Q characterising polarisation distortions is replaced by the thermo-optical constant P characterising phase distortions. It can be seen from formula (7) that a 3.6-fold increase in F (as a result of cooling to 77 K) corresponds to a 3.6-fold decrease in the parameter $\alpha P/\kappa$.

As the temperature is lowered to 109 K, the optical power in the glass MOS04 decreases by a factor of 1.7 (see Fig. 3), which means that a decrease by a factor of 1.8 can be expected at $T = 77$ K. This also corresponds to a 1.8-fold decrease in the parameter $\alpha P/\kappa$. Taking into account the results of measurements presented in Figs 2 and 3, it can be concluded that the ratio P/Q of thermo-optical constants varies insignificantly in the investigated temperature range both for the TGG crystal and the MOS04 glass.

4. Temperature dependence of the Verdet constant

Figure 1c shows the scheme of the setup for measuring the temperature dependence of the Verdet constant. Polarised radiation from ytterbium laser (*1*) passed through magnetically active element (*5*) being studied inside vacuum cryostat (*2*). Magnetic system (*10*) is located outside the cryostat and is not cooled, i.e., the magnetic field to which magnetically active element (*5*) is exposed does not vary upon a change in temperature. After passing through calcite wedge (*4*), the radiation is recorded by CCD camera (*9*). Spar wedge (*4*) is placed on an optical bench with a limb and tuned to the minimum radiation transmission at the CCD camera.

As a result of the Faraday effect, the initial linear polarisation of laser radiation passing through the magnetically active element is turned through an angle

$$\varphi = VBL, \tag{9}$$

where V is the Verdet constant and B is the magnetic induction. It is well known [16–18] that a decrease in temperature leads to an increase in the Verdet constant according to the law

$$V = \mathrm{const}/T, \tag{10}$$

i.e., $V^{-1}\mathrm{d}V/\mathrm{d}T = -1/T$. The linear expansion coefficient $L^{-1}\mathrm{d}L/\mathrm{d}T$ is negligibly small in comparison with this quantity (see Table 1) and hence, the linear expansion of the optical elements can be neglected. In the course of the experiments described in this section, the magnetic field of the system does not change and hence the observed dependence $\varphi(T)$ is determined entirely by the temperature variation of the Verdet constant.

Figure 4 shows the results of measurements of the temperature dependence of the angle of rotation of the polarisation plane in the investigated samples. For convenience of interpretation, we introduce the dimensionless parameter

$$\varphi_{\mathrm{norm}}(T) = \frac{\varphi(T)}{\varphi_0}, \tag{11}$$

where $\varphi_0 = \varphi(T_0)$. In accordance with Eqn (10), the normalised angle φ_{norm} of rotation of the polarisation plane, and hence the Verdet constant also, increase by a factor of $\sim$3.5 upon cooling to 86 K for both MOS04 glass and TGG crystal. Hence, in accordance with relation (9), cooling of any magnetically active element in the FI to 77 K helps reduce its length to nearly one-fourth.

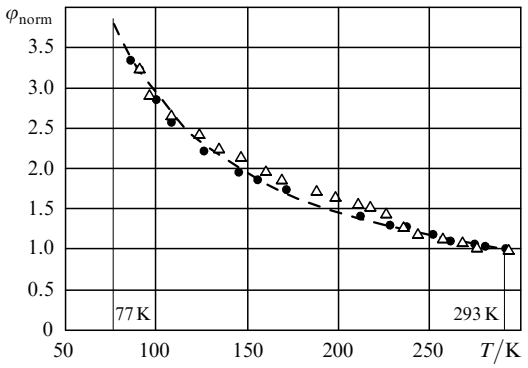

Figure 4. Theoretical (dashed curve) and experimental (symbols) temperature dependence of the normalised angle of rotation of the polarisation plane φ_{norm} in a TGG crystal (dark circles, $\varphi_0 = 4°10'$) and MOS04 glass (triangles, $\varphi = 3°$).

5. Temperature dependence of the magnetic field

All ferromagnets possess a spontaneous magnetic moment, i.e., a finite magnetisation even in zero external magnetic field [19]. The presence of spontaneous magnetisation indicates that the electron spins and magnetic moments are oriented in the substance in an ordered manner. In the absence of an external magnetic field, the magnetisation of a ferromagnet depends only on the magnetic field produced by it. The magnetic field of ferromagnetic materials is characterised by the residual magnetic induction B. It is also known that the residual magnetic induction depends linearly on the temperature T of the ferromagnet and the temperature coefficient $\alpha_B = (1/B)(\mathrm{d}B/\mathrm{d}T)$ of the residual magnetic induction is negative [20], i.e., the value of B increases with decreasing temperature.

Figure 1d shows the experimental setup used for studying the temperature dependence of the magnetic field of the magnet. Magnetic system (*10*), which is a ferromagnetic ring, was placed in cryogenic chamber (*2*) and was cooled together with magnetically active element (*5*) situated in the centre of the ferromagnetic ring. The characteristic value of

magnetic field in such a ring at the site of the crystal is ~ 5 kOe.

Figure 5a shows the results of the experiments. In order to separate the increase in the angle of rotation of the polarisation plane due to a variation of the magnetic field of the system only, the obtained results were presented in a system of coordinates in which the dashed horizontal line passing through unity (Fig. 5b) corresponds to a temperature-independent magnetic field. The results of the experiments shown in Fig. 5 are in good agreement with the results of calculations (solid curve) for the magnet Nd–Fe–B if $\alpha_B = 1.3 \times 10^{-3}$ K^{-1}.

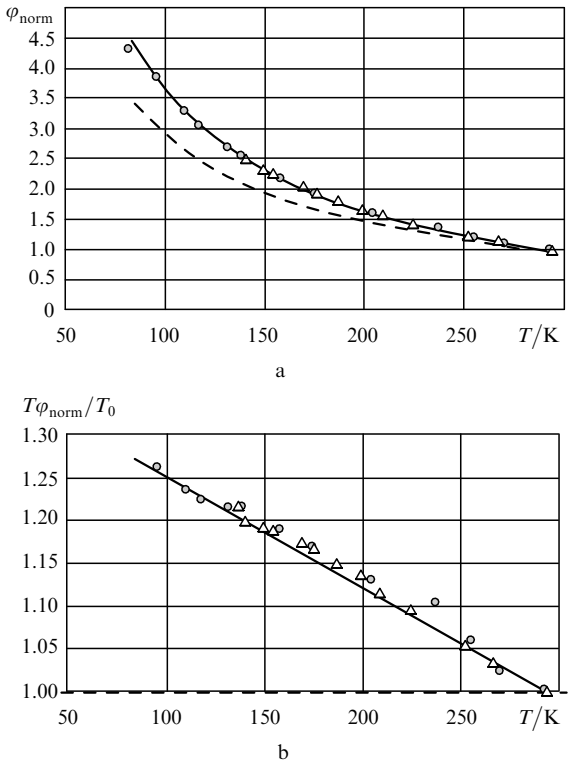

Figure 5. Theoretical (solid and dashed curves correspond to a cooled magnet and a magnet without cooling, respectively) and experimental (symbols) temperature dependences of the normalised angle of rotation of the polarisation plane.

Moreover, it was found in the course of the experiment that the experimental dependence is determined by the rate at which liquid nitrogen is supplied and by the quality of the thermal contact between the coolant and the magnetic system. It was shown as a result of a series of experiments that the largest values of the angle of rotation of the polarisation plane, which are also closest to the theoretical values, are obtained as a result of the slowest cooling of the magnets. In order to measure the dependences shown in Fig. 5, a situation was created when the temperature of the inner chamber of the cryostat was maintained at a certain constant value for a long time, after which measurements were performed. Such an experiment could be carried out over three days while a few hours were sufficient for the other experiments described above.

The results of the series of experiments show that two effects, namely, temperature dependences of the Verdet constant and magnetic field, lead to a nearly fourfold increase in the value of φ as the temperature is lowered to 93 K; in turn, this could lead to a nearly fivefold increase in the angle of rotation of the polarisation plane at 77 K. Hence, if the total length L of the magnetically active element decreases by a factor of φ upon cooling of the FI to 77 K, the depolarisation of a traditional FI ($\gamma \sim L^2$) as well as of an FI with depolarisation compensation ($\gamma \sim L^4$ [2]) will decrease considerably.

In the present research, the ferromagnet was the alloy Nd–Fe–B, which is a standard magnet used in FIs working at room temperature. In some alloys, however, the residual magnetic induction at liquid nitrogen temperature is higher (due to a larger value of α_B) than in the alloy used by us in spite of a lower value of B at room temperature. This advantage can also be used while fabricating a Faraday isolator.

6. Discussion of results

Summing up the results of our investigations, we present the estimates for the highest average power of a Faraday isolator cooled to 77 K. According to (2) and (3), the laser radiation power P_L is proportional to $\kappa/\alpha Q$ for a given value of γ. Experiments show that the parameter $Q\alpha/\kappa$ decreases by a factor of three at 77 K, while the increase in the Verdet constant and the magnetic field lower the length L of the crystal fivefold, and hence P_L increases by a factor of 15.

It must be remarked that TGG crystals are grown in two ways, viz., from the flux or from the melt. The TGG crystals used in our experiments were grown from the melt. The thermal conductivity of such crystals is practically constant in the temperature range 77–300 K [27], and hence the measured decrease in the depolarisation γ is associated with a decrease in αQ. The thermal conductivity of TGG crystals grown from the flux is double at 77 K [27], i.e., the parameter $\alpha Q/\kappa$ will be six times larger at this temperature than at 293 K. Thus, cooling of a conventional FI to 77 K can increase the average power by a factor of 30 and hence it can be used for a transmitted power of several kilowatts. Since the ratio P/Q depends weakly on temperature, all that has been said above is valid not only for isolation, but also for the emerging thermal lens.

In the case of an FI with depolarisation compensation, the 30-fold gain is augmented by a decrease in ξ (see above), since in such FIs $\gamma_{\min}$ depends on ξ, its value being lower for smaller values of ξ [2]. According to Fig. 2 and expression (5), we can expect a ~ 1.9-fold decrease (from 2.25 to 1.2) in the value of ξ at 77 K. In this case, the maximum power increases further by a factor of 1.6 [2]. Since such FIs may operate at room temperatures for a radiation power of 1–2 kW, a maximum power of 100 kW can be expected at $T = 77$ K.

The above results pertain to a rod geometry, i.e., to the case when the magnetically active element is cooled through its side surface. The characteristic length of a TGG crystal in FI cooled to 77 K is 3–4 mm, which is one-fifth of its length at room temperature. This allows us to use the disc geometry in which the magnetically active element is cooled through the optical surfaces with the help of, for example, sapphire. Such a method was used successfully in the active elements of lasers [15]. Preliminary experiments carried out by us also revealed a considerable decrease in depolarisation that is in complete accord with the predictions of the theory [11].

Naturally, the fabrication of cryogenic Faraday isolators involves a whole range of complications. These include the need for constructing magnetic systems with specific configurations, the presence of a cryogenic chamber, liquid nitrogen filling, etc. However, these are technical difficulties that can be overcome. There are no basic physical problems hindering a progress towards the 100-kW power range.

References

1. Zarubina T.V., Petrovskii G.T. *Opt. Zh.*, **59**, 48 (1992).
2. Khazanov E.A. *Kvantovaya Elektron.*, **26**, 59 (1999) [*Quantum Electron.*, **29**, 59 (1999)].
3. Abramovici A., Althouse W.E., Drever R.W.P., Gursel Y., Kawamura S., Raab F.J., Shoemaker D., Sievers L., Spero R.E., Thorne K.S., Vogt R.E., Weiss R., Whitcomb S.E., Zucker M.E. *Science*, **256**, 325 (1992).
4. Khazanov E.A. *Kvantovaya Elektron.*, **30**, 147 (2000) [*Quantum Electron.*, **30**, 147 (2000)].
5. Mueller G., Amin R.S., Guagliardo D., McFeron D., Lundock R., Reitze D.H., Tanner D.B. *Classical and Quantum Gravity*, **19**, 1793 (2002).
6. Khazanov E.A., Andreev N.F., Mal'shakov A.N., Palashov O.V., Poteomkin A.K., Sergeev A.M., Shaykin A.A., Zelenogorsky V.V., Ivanov I., Amin R.S., Mueller G., Tanner D.B., Reitze D.H. *IEEE J. Quantum Electron.*, **40**, 1500 (2004).
7. Khazanov E.A., Zelenogorsky V.V., Shaykin A.A., Kamenetsky E.E., Palashov O.V. *Proc. SPIE Int. Soc. Opt. Ing.*, **5975**, 167 (2006).
8. Khazanov E., Andreev N., Babin A., Kiselev A., Palashov O., Reitze D. *J. Opt. Soc. Am. B*, **17**, 99 (2000).
9. Khazanov E.A. *Kvantovaya Elektron.*, **31**, 351 (2001) [*Quantum Electron.*, **31**, 351 (2001)].
10. Khazanov E.A., Anastasiyev A.A., Andreev N.F., Voytovich A., Palashov O.V. *Appl. Opt.*, **41**, 2947 (2002).
11. Mukhin I.B., Khazanov E.A. *Kvantovaya Elektron.*, **34**, 973 (2004) [*Quantum Electron.*, **34**, 973 (2004)].
12. Yasuhara R., Kawashima T., Furukawa H., Ikegawa T., Matsumoto O., Sekine T., Kurita T., Kan H., Kawanaka J., Norimatsu T., Izawa Y. *Proc. Int. Symp. on Topical Problem of Nonlinear Wave Physics* (St.Petersburg – N.Novgorod, 2005) p. 135.
13. Ripin D.J., Ochoa J.R., Aggarwal R.L., Fan T.Y. *Opt. Lett.*, **29**, 2154 (2004).
14. Backus S., Bartels R., Thompson S., Dollinger R., Kapteyn H.C., Murnane M.M. *Opt. Lett.*, **26**, 465 (2001).
15. Tokita S., Kawanaka J., Fujita M., Kawashima T., Izawa Y. *Appl. Phys. B*, **80**, 635 (2005).
16. Barnes N.P., Petway L.P. *J. Opt. Soc. Am. B*, **9**, 1912 (1992).
17. Davis J.A., Bunch R.M. *Appl. Opt.*, **23**, 633 (1984).
18. Zarubina T.V., Kim T.A., Petrovskii G.T., Smirnova L.A., Edel'man I.S. *Optiko-mekh. Promysh.*, (11), 33 (1987).
19. Kittel C. *Introduction to Solid State Physics* (New York: Wiley, 1996).
20. Al'tman A.B., Vernikovskii E.E., Gerberg A.N., Gladyshev P.A., Gratsianov Yu.A., Zein E.N., Kavalerova L.A., Pyatin Yu.M., Sasatunov Yu.S., Sergeev V.G., Skokov A.D., Sukhorukov R.Yu., Chernyavskaya A.M. *Postoyannye magnity: Spravochnik* (Handbook on Permanent Magnets) (Moscow: Energiya, 1980).
21. Akhiezer A.I., Akhiezer I.A. *Elektromagnetizm i elektromagnitnye volny: Uchebnoe posobie dlya vuzov* (Electromagnetism and Electromagnetic Waves: Textbook for Universities) (Moscow: Vysshaya shkola, 1985).
22. Khazanov E.A., Kulagin O.V., Yoshida S., Tanner D., Reitze D. *IEEE J. Quantum Electron.*, **35**, 1116 (1999).
23. Khazanov E., Andreev N., Palashov O., Poteomkin A., Sergeev A., Mehl O., Reitze D. *Appl. Opt.*, **41**, 483 (2002).
24. Mezenov A.V., Soms L.N., Stepanov A.I. *Termooptika tverdotel'nykh lazerov* (Thermal Optics of Solid State Lasers) (Leningrad: Mashinostroenie, 1986).
25. Vlasov S.N., Petrishchev V.A., Talanov V.I. *Izv. Vyssh. Ucheb. Zaved. Ser. Radiofizika*, **14**, 1353 (1971).
26. Potemkin A.K., Khazanov E.A. *Kvantovaya Elektron.*, **35**, 1042 (2005) [*Quantum Electron.*, **35**, 1042 (2005)].
27. Slack G.A., Oliver D.W. *Phys. Rev. B*, **4**, 592 (1971).
28. Wynands R., Diedrich F., Meschede D., Telle H.R. *Rev. Sci. Instr.*, **63**, 5586 (1992).
29. Mansell J.D., Hennawi J., Gustafson E.K., Fejer M.M., Byer R.L., Clubley D., Yoshida S., Reitze D.H. *Appl. Opt.*, **40**, 366 (2001).
30. Chen X., Galemezuk R., Salce B., Lavorel B., Akir C., Rajaonah L. *Solid State Commun.*, **110**, 431 (1999).
31. Popov P.A. *Ph.D. Thesis* (Bryansk: Petrovskii State Education Institute, 1993).
32. Andreev N.F., Babin A.A., Zarubina T.V., Kiselev A.M., Palashov O.V., Khazanov E.A., Shchavelev O.S. *Opt. Zh.*, **67**, 66 (2000).
33. Zarubina T.V. *Private communication* (2000).